Evaluating the efficacy of solar chimneys for heating and cooling: A case study

Jan-Hendrik Grobler (CSIR)

Dirk Conradie (CSIR)

Llewellyn van Wyk (CSIR)

Background

The Department of Science and Technology (DST) together with the Eastern Cape Department of Education (ECDOE) are co-funding the construction of a science centre in the village of Cofimvaba in the Eastern Cape. The purpose of the science centre is to promote the study of science, technology, engineering and mathematics (STEM) in the school district.

The Council for Science and Industrial Research (CSIR) was appointed as DST's Implementing Agent for the project. The express purpose of this appointment was to pilot, evaluate and demonstrate the application and efficacy of innovative building technologies (IBTs) on the project in accordance with a South African Government Cabinet Resolution of August 2013 regarding the application of IBTs in government projects.

A key objective is to apply IBTs to enhance the economic, social, environmental and institutional sustainability of public buildings. For this project attention is focused on achieving net-zero energy and water consumption, and reducing waste water disposal and construction waste. A key strategy to achieve a net-zero building was to eliminate reliance on mechanical heating and cooling.

Context

The Aeronautics Systems Competency (ASC) within the Defence, Peace, Safety and Security (DPSS) Competency Area of the CSIR was requested to evaluate a concept design for a passive ventilation system for the science centre (Figure 1).

Figure 1: Science centre with the solar chimneys (circled in red) incorporated in the ventilation system (CSIR 2018)

Solar chimneys, also known as thermal chimneys, are an attractive option for naturally ventilating buildings by using convection of air heated by passive solar energy. Due to its passive operation it is able to potentially lower operational costs, reduced energy consumption and a smaller carbon footprint. The chimney provides a large plenum where ambient air is heated by the sun. As a result, the air density lowers and buoyancy forces carries it upward drawing replacement air from the building.

Significant research has been done on solar chimneys since the 1990s, using experimental, numerical or analytical approaches (or a combination). Khanal and Lei presented a comprehensive overview of solar chimney research, referencing more that 40 papers published from 1990 to 2010 [Khanal & Lei, 2011]. Computational Fluid Dynamics (CFD) was employed in 39% of the solar chimney investigations, either as the only approach or in combination with experimental or analytical methods. They found that the use of CFD modelling in solar chimney studies was increasing, no doubt due to more powerful and affordable computer hardware becoming available.

Some researchers develop their own CFD codes for their analysis [Imran et al, 2015], but the use of commercial CFD software remain a very popular option. Many general purpose CFD codes are available with FLUENT (recently bought by ANSYS) and STAR-CCM+ (recently bought by Siemens) dominating the market.

Researchers generally use a similar approach. Solar heating on the absorber wall is modelled either as isoflux or isothermal heating; walls are specified as no-slip; second-order upwind differencing is the scheme of choice for solving the momentum, energy and turbulence transport equations and under-relaxation factors are used to ensure numerical stability [Khanal & Lei, 2006].

The k-epsilon turbulence model is available in almost all commercial CFD codes and frequently employed in solar chimney models. Experimental data can be matched withing 2% [Harris et al, 2007] although results within 15% may also be deemed acceptable [Lei et al, 2016].

Meshes of fewer than 1 million cells are generally sufficient to model the chimney region. For example, Lei found results varied by less than 2% between meshes consisting of approximately 304 000 and 357 000 cells [Lei et al, 2016] while Suárez-López found negligible differences in meshes varying in size from 100 000 to 2 million cells [Suárez-López et al, 2015].

Methodology

The commercial CFD code, STAR-CCM+, was used to analyse the flow in a model of the science centre on a typical summer and winter day. The model was designed in accordance with the general approach outlined above. Simulations were performed on the 276-CPU computer cluster of the CFD facility of CSIR.

The analysis was performed in two phases. In the initial phase, a simplified model of the chimney region only was simulated in order to obtain realistic chimney wall temperatures. These temperatures were then used as input for the next phase where the model was extended to include the relevant parts of the building and environment.

Phase 1: Chimney-only models

The temperature reached by an external surface, for example the roof of a building, can be estimated by evaluating the balance between the energy absorbed from the sun and the energy radiated back to the sky, assuming steady state conditions and ignoring any transmission of energy to the interior.

The inputs required are:

- Solar radiation reaching the roof surface (W/m^2)
- Solar absorptance coefficient of the roof surface
- Solar emittance coefficient of the roof surface
- Convective heat transfer coefficient resulting from airflow over the roof surface (W/m^{2}K)
- Sky temperature (°C or K)
- Ambient air temperature (°C or K)

The sky temperature (in Kelvin) can be estimated with the following empirical formula which is valid in the range -20°C to 30°C (Lienhard et al., 2008):

$$T_{sky} = T_{air}\left[0.711 + 0.0056T_{dp} + 7.3 \times 10^{-5}T_{dp}^2 + 0.013\cos(2\pi t/24)\right]^{\frac{1}{4}} \quad (1)$$

Where:

T_{air} = Air temperature in Kelvin

T_{dp} = Dew point temperature in °C

Calculations based on this method were used to validate the chimney-only CFD model. The chimney-only CFD model consisted of a solid region, representing the carbon steel chimney walls, and a fluid region, representing the air present on the inside and outside of the chimney. An inlet and outlet flow boundary allowed air to flow through the chimney along the z-axis. (Figure 2). Radiation energy entered and left the domain through two additional boundaries (along the y-axis in Figure 2). The

model was designed to simulate a representative section of the chimney wall and did not attempt to account for corner effects. It could therefore extend any distance along the x-axis in Figure 2. The chimney-only model consisted of 287 040 cells (283 600 fluid cells and 3 440 solid cells).

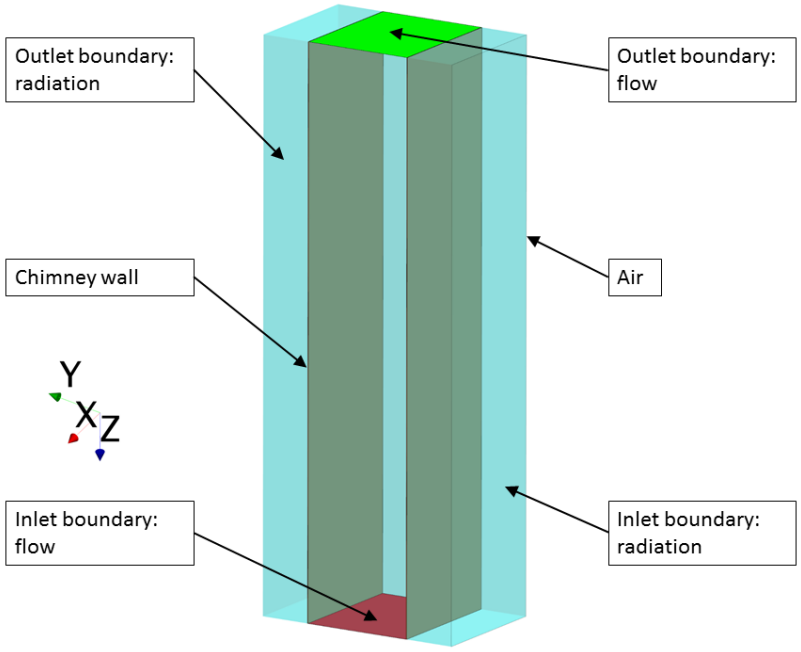

Figure 2: Chimney-only model

The results obtained from the CFD chimney-only model and estimates based on the calculations compared well. Simulations were performed with a solar absorptance coefficient of 0.9 and 0.26. The CFD model predicted roof temperatures of 57.3 °C and 35.7 °C for the higher and lower value respectively, compared to the calculated values of 65 °C and 39 °C, respectively.

The chimney-only model was then used to obtain chimney wall temperatures for the relevant chimney surfaces on the days selected for simulation.

Phase 2: Extended models

The extended model included not only the chimney, but also the lecture rooms, connecting passages and a part of the environment, as shown in Figure 3.

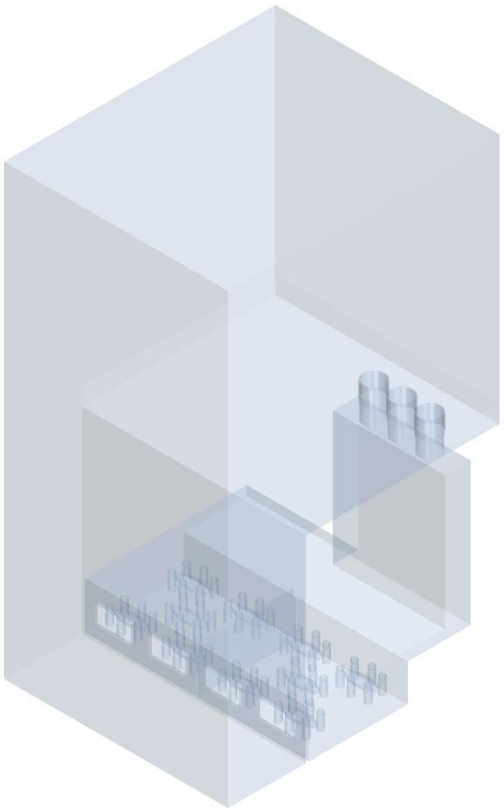

Figure 3: Extended CFD-model including the chimney, lecture room and environment

The analysis required the solution of a buoyancy driven flow problem. Hot air in the chimney rises and is replaced by ambient air drawn through the lecture room windows. The air passes though the lecture rooms and enters a passage at ceiling level which is connected to the chimney. The CFD model was a closed loop system: the air expelled from the chimney returned to the region where the windows were located, cooled along the way to approximate the desired ambient air temperature.

To support the various calculations such as solar radiation and the solar angles at critical times a typical meteorological year weather was generated with the *Meteonorm v7.2.4* software using typical meteorological years based on statistically interpolated data and satellite data for solar radiation. Unfortunately there are no official measured weather stations in this deep rural area. The weather file is for the 2009 climate.

Two critical days were selected for analysis: the hottest day of the year and the coldest. The available weather data indicated that statistically, these days were 1 January (hottest) and 16 July (coldest) with peak ambient air temperature of 32.989 °C and 16.547 °C, respectively. Figure 4 and 5 show the available weather data for 1 January and 16 July, respectively. *Ecotect v5.60* was used to determine these two days.

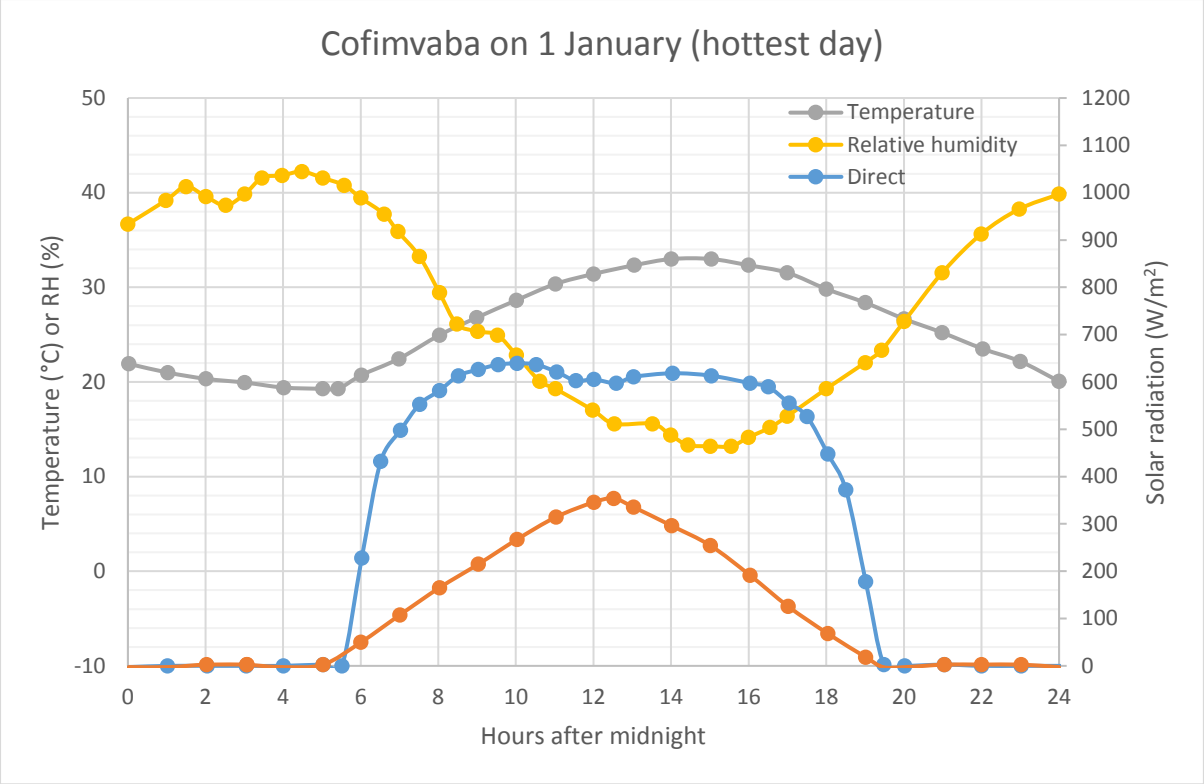

Figure 4: Weather data for 1 January (CSIR 2018)

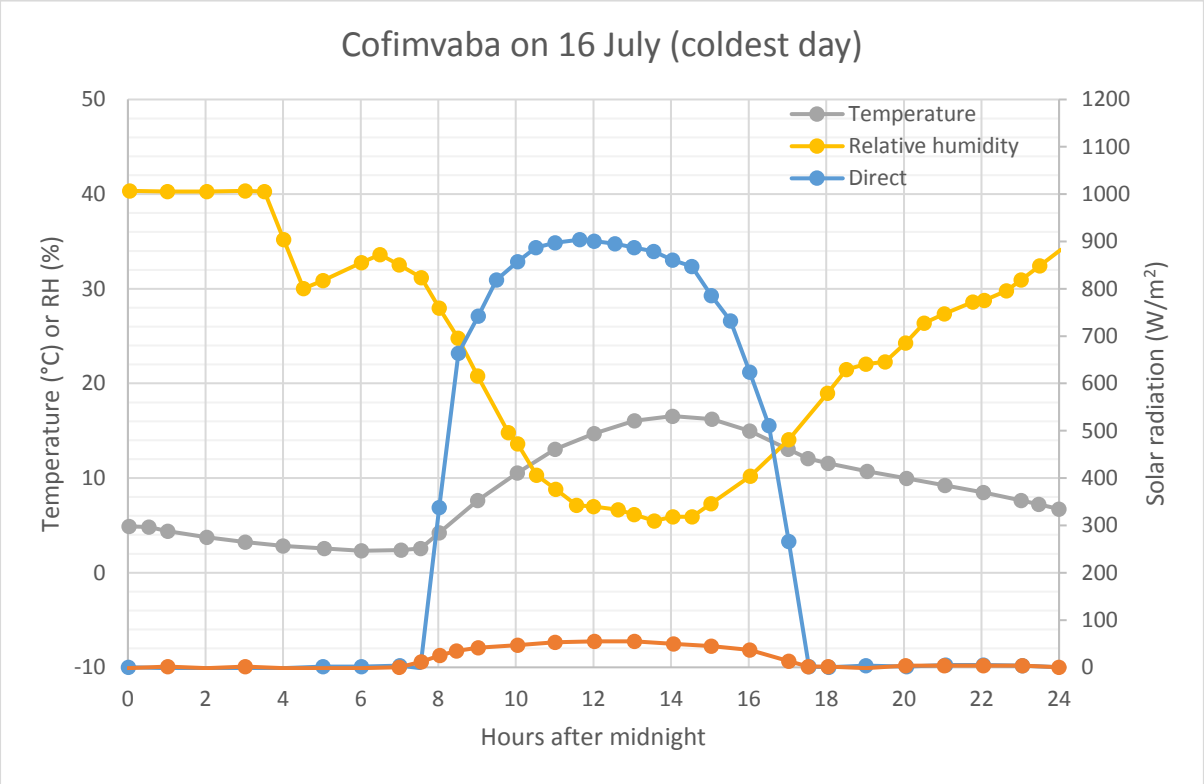

Figure 5: Weather data for 16 July (CSIR 2018)

In addition to the direct and diffuse solar radiation, the sun angles were also available every hour on the hour. The sun angles were calculated by means of a bespoke new Early Design Phase (EDP) experimental software platform (developed by author) that uses as its input a typical meteorological

year weather file, and combines it with advanced algorithms to calculate the solar azimuth and elevation for each of the 8 760 hour data records in the weather file. The base 8 760 data points have been interpolated by means of a La Grange polynomial interpolation routine to 35 037 datapoints to ensure a less granular solar exposure diagram. The solar energy available on the walls of the solar chimney could be calculated with this data. The sun angles were given as the azimuth (in degrees clockwise from north) and elevation (in degrees with horizontal as 0°).

The effective direct solar radiation on a surface will depend on the angle between the incoming rays and the surface normal. If the angle of the incoming radiation and the surface normal are known, the angle between them can be obtained by evaluating the scalar product of the vectors. This angle can then be used to determine the effective solar radiation on the surface.

For two 3-dimensional (3D) vectors, $a = [a_1; a_2; a_3]$ and $b = [b_1; b_2; b_3]$ the scalar product can be calculated in one of two ways:$a \cdot b = a_1 b_1 + a_2 b_2 + a_3 b_3$
(2)

or:

$$a \cdot b = \|a\|\|b\| \cos\theta \quad (3)$$

where θ is the angle between the vectors.

By combining these equations, the angle between the vectors can be determined. If the radiation hits the surface perpendicular, the surface normal and a vector pointing towards the position of the sun both point in the same direction (i.e. θ = 0°). A ray bundle with a unit area cross section will be spread over the same area on the surface, i.e. there will be no dilution of the radiation intensity. At any other angle, the rays from the unit area cross section will be spread over a larger-than-unit area on the surface, resulting in an effective dilution of the radiation energy. The extent of the dilution effect can be determined by geometric considerations, as shown in Figure 6.

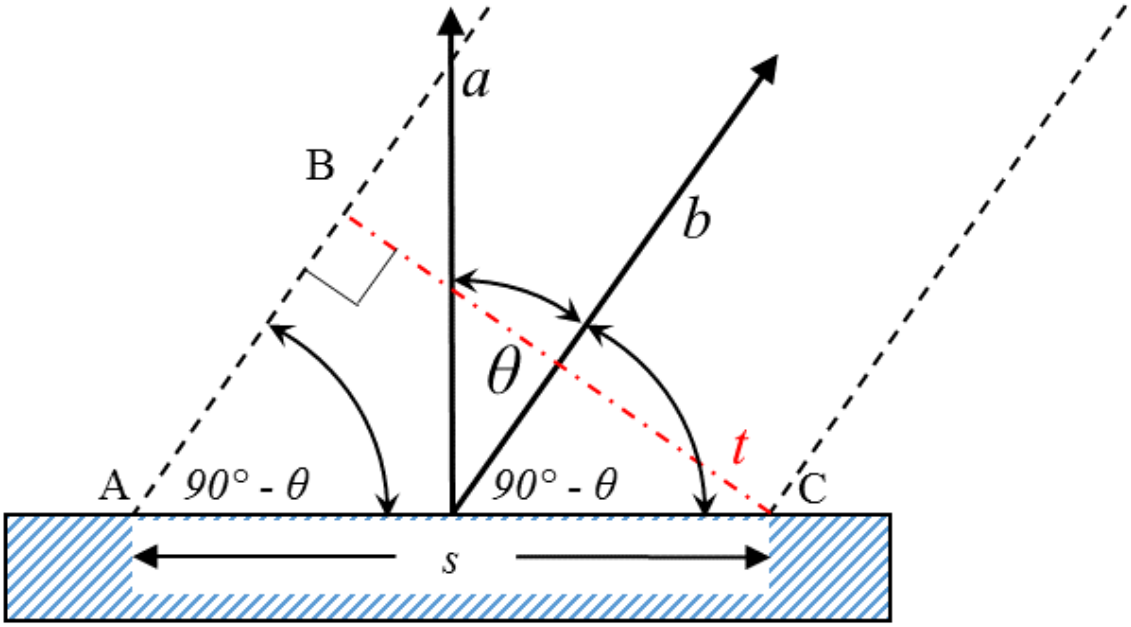

Figure 6: Solar radiation entering through unit area, t, is distributed over surface, s

In Figure 6, side t (in red) represents a unit area perpendicular to the ray bundle and side s represents the surface area over which the radiation energy is spread when it hits the surface. Vector b points in the direction of the sun vector a normal the surface.

Consider right triangle ABC in Figure 10:

$$\sin(90° - \theta) = \frac{t}{s} = \cos\theta \quad (4)$$

The effective direct solar radiation is therefore given by $\cos\theta$. If rays hit the surface perpendicular (i.e. θ = 0°) $\cos\theta$ = 1 and 100% of the available radiation per unit area hits a unit area on the surface. At 60° for example, $\cos\theta$ = 0.5 and only 50% of the available radiation per unit area will reach a unit area on the surface.

Results

Hottest day (1 January)

The method outlined above along with solar radiation data from weather files were used to obtain solar loads on the relevant surfaces of the chimney wall which in turn, were used as input to the chimney-only model to obtain surface wall temperatures. The results obtained for 1 January are shown in Table 1, below.

Table 1: Surface temperatures obtained from chimney-only model for 1 January

Surface	Temperature (°C)
West	54.03
South	41.56
Top	69.17

The temperatures were applied to the relevant wall boundaries in the extended model and simulations were performed. In addition to the chimney walls, heat could also enter the domain through the people present in the lecture rooms. A total of 60 people were modelled (30 in each of the lecture rooms) adding and average of 100 W metabolic energy per person.

The part of the building that was modelled contained two rooms: one directly adjacent to the chimney (Room A) and one not directly adjacent (Room B). Room B had a slightly higher temperature than the Room A at ceiling level, as seen in Figure 12. This slight difference can be attributed to lower velocities in the region above Room B which in turn is due to the layout of the building. The shortest route from Room A to the chimney leads through a passage with a cross section of approximately 4.3 m^2 while air from Room B must cross a section with an area of approximately 2.4 m^2. This section can be subdivided in a subsection with an area of approximately 1 m^2 where most of the air from Room B could easily reach the chimney and a subsection of approximately 1.4 m^2 where it has to join the air from Room A for access to the chimney inlet. Due to these factors Room B would experience significantly more resistance to reach the chimney inlet and as a result, a larger part of the outside air will pass through Room A to reach the chimney (Figure 7).

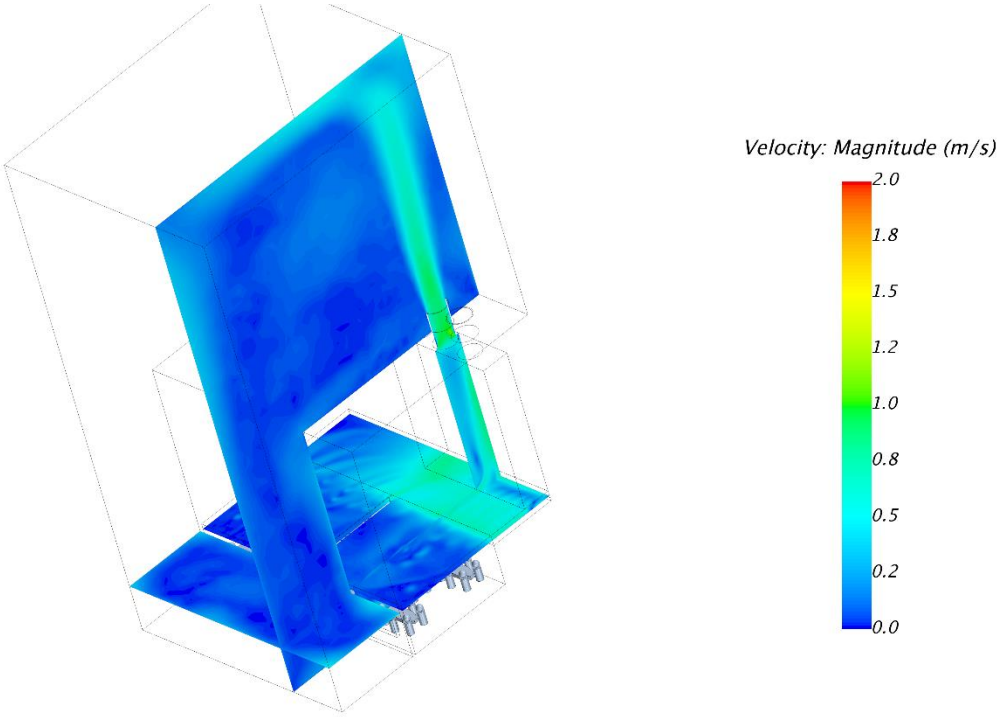

Figure 7: Velocities at ceiling level and through centre chimney outlet

Velocity vectors in the lower region of the chimney is shown in Figure 8. The vectors are coloured by their magnitude. A recirculation zone is clearly visible at the bottom of the chimney. The momentum of the air entering the chimney carries it to the outer wall where it remains as it ascends.

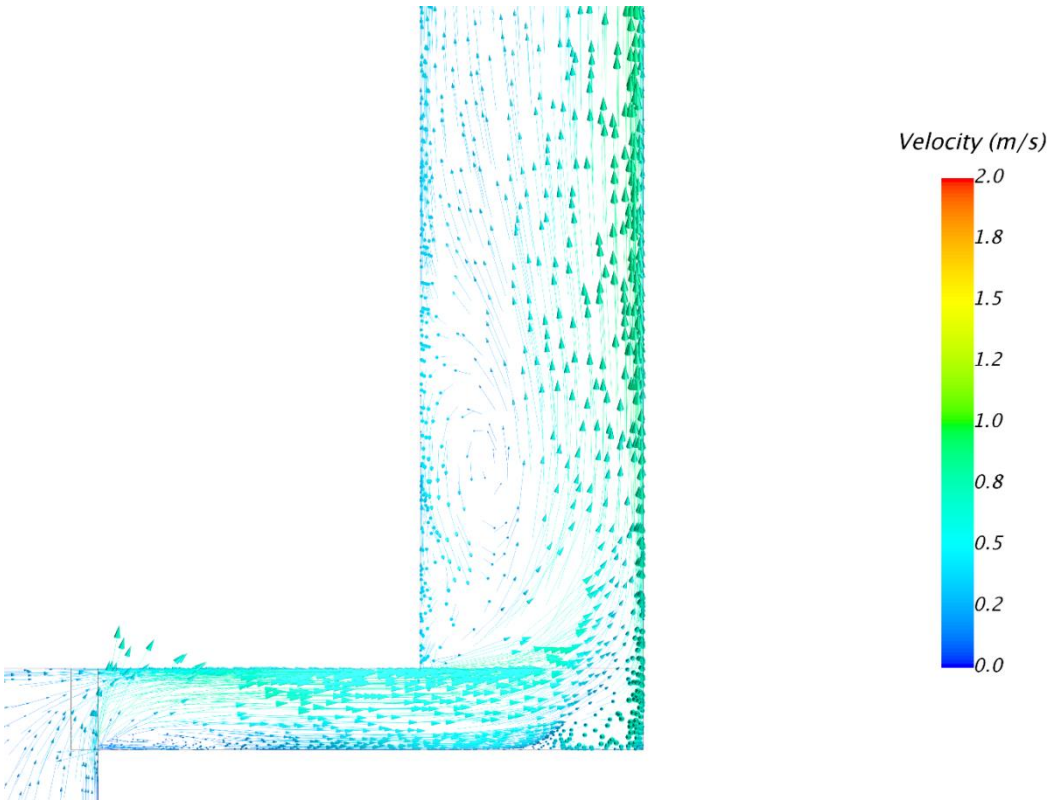

Figure 8: Recirculation zone in lower part of chimney

Simulating the hottest day of the year (statistically) at the hottest time of the day (14:00) gave the performance in a best case scenario. Results indicated that the chimney would perform quite well under such circumstances. The predicted air change rate was approximately 41, which is relatively high. Significant air flow is drawn in through the windows, with maximum air speeds of approximately 0.55 m/s, which is also relatively high. Given that the ambient air temperature on that day was almost 33 °C such speeds are welcomed as it would help evaporatative cooling effect over the skin.

The main aim of the simulations were to firstly determine if the solar chimney will work adequately and secondly to give an indication of how well it could work. The model predicted that the chimney will work very well in a best case scenario. It is understood that the performance of the chimney in real-life conditions will vary between this optimum performance point and a minimum where it is not expected to work at all. For example, the chimney is not expected to function at all is during overcast or rainy days.

Coldest day (16 July)

In winter, it is expected that the windows of the lecture rooms will be shut tight which implies that no through flow of air is possible in the lecture rooms or chimney. The chimney could still be of benefit if hot air could be drawn from its plenum into the lecture rooms. This scenario was modelled by making minor adjustments to the extended model.

Hot air will have to be drawn from the chimney into the lecture rooms by mechanical means. No information was available regarding the size of any fans, their characteristics or where they would be located. It was assumed that all windows would be closed but that some air would still leave the domain due to seepage. For the purpose of the simulation four air changes per hour (ACH) were selected to account for this effect: 0.5, 1, 2 and 4.

The closed loop system where air that exits the chimney eventually re-enters the windows was interrupted and the windows were instead specified as outlets and air was allowed to enter the domain through a pressure boundary. The selected ACH were specified at the window boundaries. Figure 9 shows the location on the boundaries in the modified model.

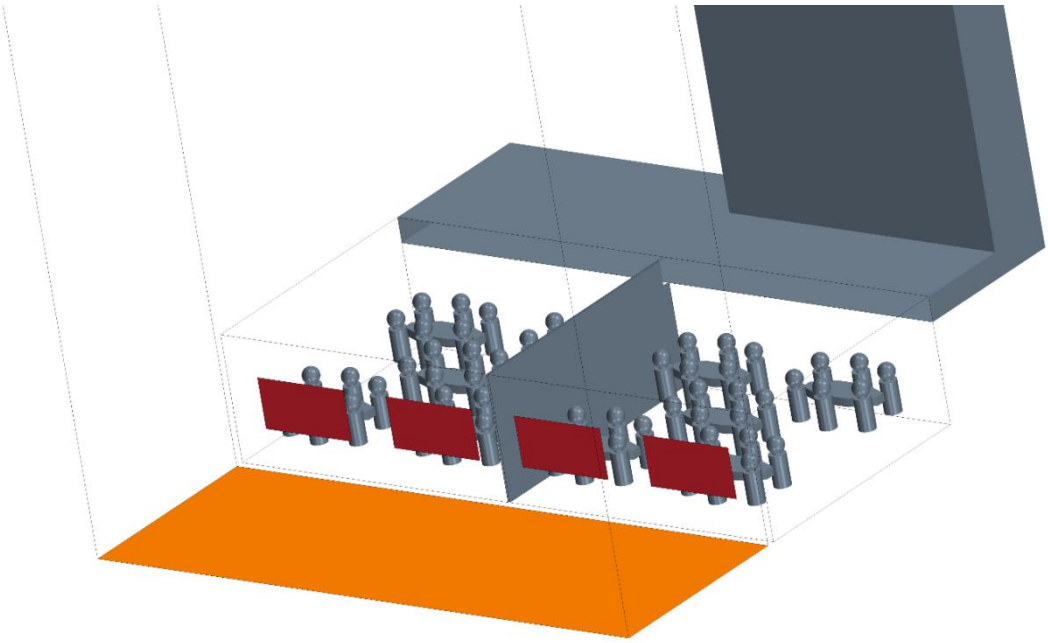

Figure 9: Location of boundaries in modified model: outlet (red) and pressure (orange)

Simulations similar to those used to generate the results shown in Table 1 were performed using weather data and solar angle inputs for the coldest day of the year, which was 16 July (statistically). The results obtained are shown in Table 2.

Table 2: Surface temperatures obtained from chimney-only model for 16 July

Surface	Temperature (°C)
West	48.40
North	28.28
Top	28.80

These temperatures were applied do the relevant wall boundaries in the (modified) extended model and simulations were performed. Figures 10 and 11 show some of the key features of the flow in the building.

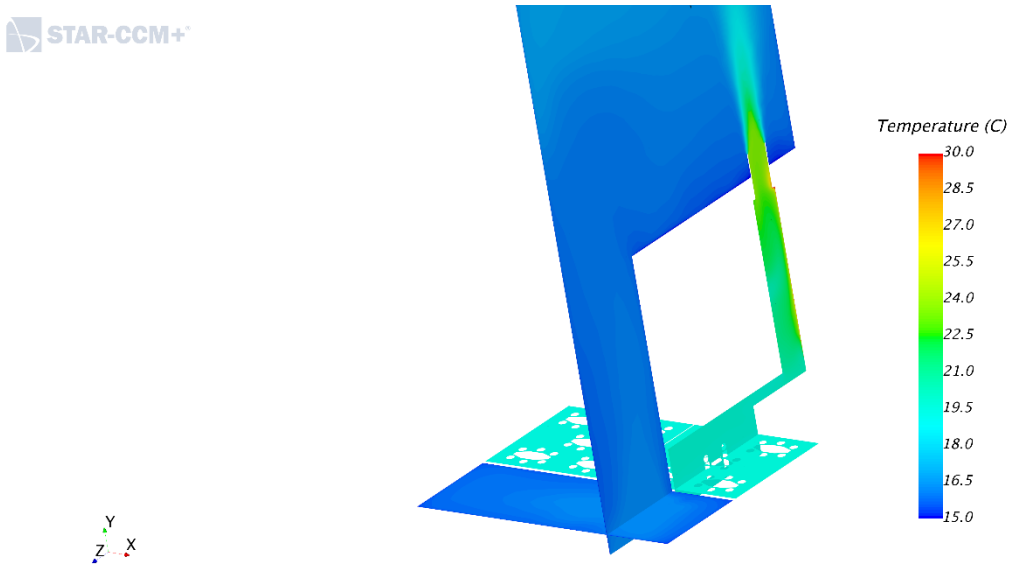

Figure 10: Temperature distribution in building with 4 ACH ventilation rate

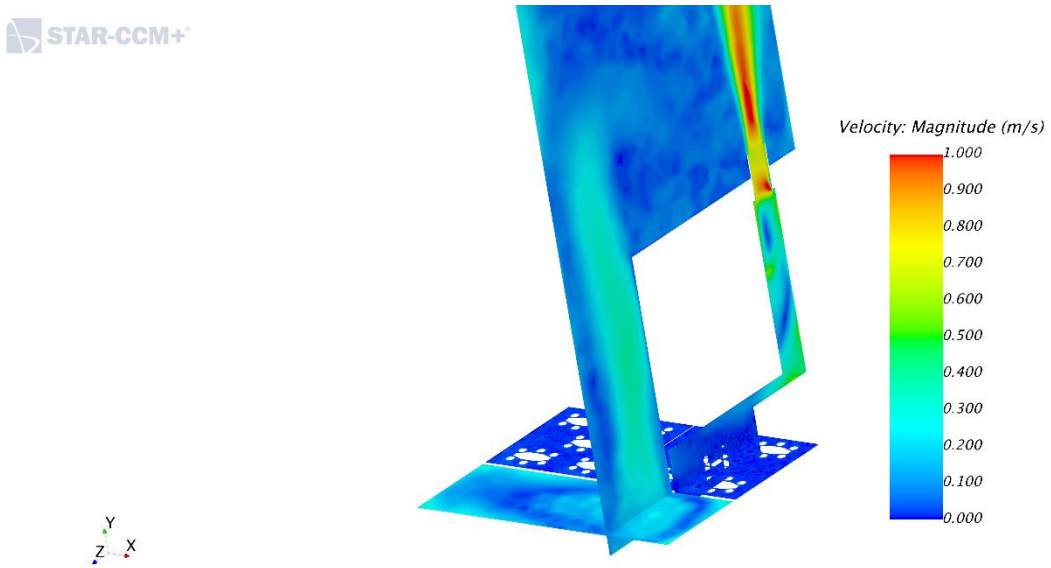

Figure 11: Velocity distribution in building with 4 ACH ventilation rate

The results show that the increase in room temperature due the extraction of hot air from the chimney seem to reach a limit, as shown in Figure 12. The outside air (at 16.21 °C) is heated to approximately 19.23 °C after passing through the chimney at 1 ACH.

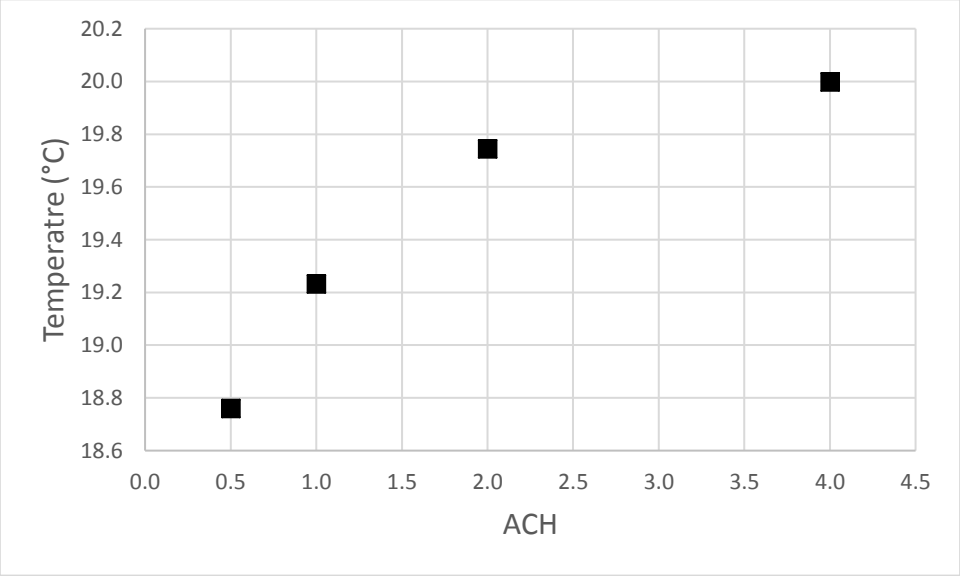

Figure 12: Average temperature in lecture rooms as a function of ventilation rate

Conclusion

The concept design for a passive ventilation system for the science centre was simulated using commercially available CFD software. A hot summer day and a cold winter day were simulated. The results indicated that a maximum ACH of 41 is possible under favourable conditions in summer while ambient air drawn through the chimney at a rate of 1 ACH could be heated from 16.21 °C to 19.23 °C on a cold winter day.

The simulations indicate that a solar chimney can perform well in the particular climatic conditions.

References

Harris, D. and Helwig, N. 2007. “Solar chimney and building ventilation.” *Applied Energy* 84 (2007) 135-146.

Imran, A., Jalil, J., and Ahmend, S. 2015. “Induced flow for ventilation and cooling by a solar chimney.” *Renewable Energy* 78 (2015) 236-244.

Khanal, R. and Lei, C. 2015. “A numerical investigation of buoyancy induced turbulent air flow in an inclined passive wall solar chimney for natural ventilation.” *Energy and Buildings* 93 (2015) 217-226.

Khanal, R. and Lei, C. 2011. “Solar chimney – A passive strategy for ventilation.” *Energy and Buildings* 43 (2011) 1811-1819.

Khanal, R. and Lei, C. 2014. “An experimental investigation of an inclined passive wall solar chimney for natural ventilation.” *Solar Energy* 107 (2014) 416-474.

Lei, Y., Zhang, Y., Wang, F. and Wang, X. 2016. “Enhancement of natural ventilation of a novel roof solar chimney with perforated absorber plate for building energy conservation.” *Applied Thermal Engineering* 107 (2016) 653-661.

Suarez-Lopez, M., Blanco-Marigorta, A., Gutierrez-Trashorras, A., Pistona-Favero, J. and Blanco-Marigorta, E. 2015. “Numerical simulation and exergetic analysis of building ventilation solar chimneys.” *Energy Conservation and Management* 96 (2015) 1-11.